PS depth imaging to detect clastic reservoirs --Vietnam's first 3D-4C OBC survey in the Cuu Long Basin.

Fong Cheen Loh, Boon Leng Chuah, Zhen Yu Zhou, Jian Cai, Xue Gong, Jian Feng Yao, Xiao Gui Miao, Joe Zhou, CGG, Nguyen Lam Anh, Vu Van Khuong, Vietsovpetro

Summary

Fractured granite basements are the main producing reservoirs in the Cuu Long basin, Vietnam. Besides these historical main targets, some oil discoveries have been found in the Oligocene-Miocene clastic layers. Among them, some can be identified in PP wave images, while others may lack sufficient P impedance contrasts, and thus can be difficult to find. PS waves respond to lithology and pore saturation changes differently from PP waves, and therefore are capable of providing additional geological information for identifying potential reservoirs in clastic layers. In addition, PS seismic data can be used for PP-PS joint AVO inversion to improve reservoir definition and reduce uncertainties in hydrocarbon prospect evaluation.

In this study, efforts have been invested in the PS wave time and depth processing and imaging in order to obtain high quality images and extract important reservoir and lithology information. We highlight some key processing steps such as surface wave inversion, shear wave splitting analyses, PS wave demultiple and joint PP/PS velocity model building.

Introduction

Block 09-1, Cuu Long Basin, is located near the port of Vung Tau, offshore Vietnam. An OBC 3D4C survey, with a total full fold area of 847 sqkm, was designed to improve the imaging of the clastic and fractured reservoirs inside the deep basement. Despite the successful basement exploration and development in the Cuu Long Basin, the future will also involve exploration of the younger clastic stratigraphy for increased oil recovery. It is challenging to see the details of the rock types, structures, and saturation in clastic layers using 3D depth images from PP waves alone. This is because PP waves respond similarly to the different rock types present here and therefore may see only weak impedance contrasts at some key interfaces. PS waves, on the other hand, can provide complementary images to characterize the rock structures and fluid boundaries, thus helping to characterize potential reservoir zones. Since PS processing is more complex and difficult than PP processing, several challenges had to be addressed to obtain reliable PS image such as huge statics caused by near surface shear velocity variations, (directional) shear wave splitting, complex multiples from both P and S legs, and the need for an accurate velocity model to match PP and PS seismic events for interpretation (Figure 1). We first explain our strategies to resolve these processing challenges and then with the data example we show that the reservoir reflectivity is well resolved in the PS image but not in the conventional PP image. We also show that seismic amplitudes and velocities can be used to locate the prospective pay inside these secondary reservoir zones. Finally, the advantages of PP-PS joint AVO inversion are demonstrated.

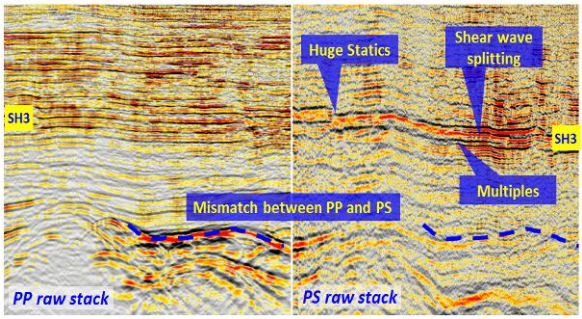

Figure 1: Raw PP and PS stack with minimum denoising.

Surface wave modeling and inversion for velocities and statics

Surface waves can be useful signals in building a near surface velocity model that can then be used for PS statics correction. Miao et al. (2016) presented a robust non-linear multi-modal surface wave inversion by utilizing a differential evolution algorithm to minimize the difference between the modeled and observed surface wave dispersion spectra to invert for shallow velocity models. The workflow involves multi-offset dispersion analysis, automatic dispersion-curve picking, and multi-modal inversion as shown in Figure 2A. In this survey, the rough sea floor varies from sharp emerged reefs to high absorptive flood alluvial fans which results in large shear statics in the PS data. The conventional shear statics correction method requires human picking/registration of PP/PS horizons, which is not only hard to ensure event consistency between PP and PS images but also difficult to manage for such a large OBC survey. Surface wave inversion in this case provides a more manageable solution for shear statics corrections (Miao et al., 2016). An example of using the inverted Vs model to compute shear statics which are then applied to the PS data is shown in Figures 2B and 2C. After application of shear statics the lateral coherency and continuity of the reflection events are significantly improved, verifying the reliability of the inverted shallow Vs model.

Clastic reservoir detection through 3D-4C PS imaging in Cuu Long Basin, Vietnam

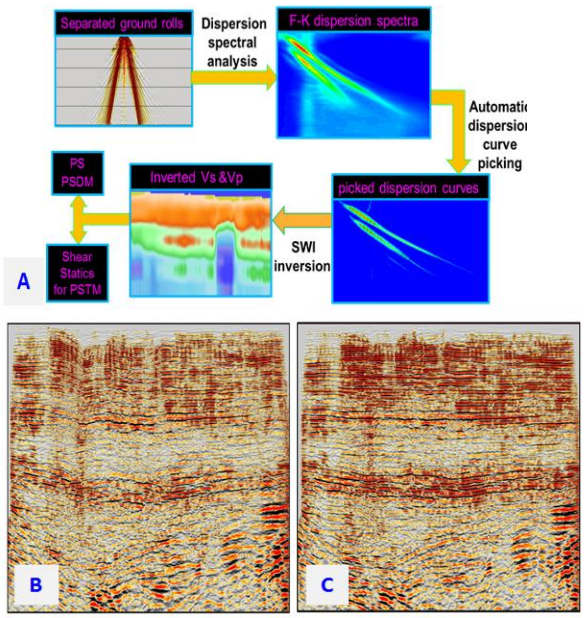

Figure 2: (A) Surface wave inversion (SWI) workflow, (B) Stack section before SWI shear statics applied; (C) Stack after SWI shear statics applied.

Shear wave splitting

The particle motions of P waves are polarized parallel to the propagation direction while S waves are polarized perpendicular to the propagation direction. When the polarized shear wave enters an anisotropic medium, it splits into two independently polarized waves according to the anisotropy (stress or fracture-induced) orientation. The differences in wave speed for these two modes causes them to become separated in time and thus the waves carry the imprint of the anisotropic medium (Bale, et al., 2009).

Such shear wave splitting can degrade the resolution and amplitude of the PS wave image significantly. Fortunately, we can compensate for this splitting effect by calculating the time delay between fast (S1) and slow (S2) waves and then applying the shifts on prestack data to align all S2 traces to S1. Shear wave splitting also opens a window into the analysis of fracture density and orientation, which can be important for well locations, injection and horizontal drillings. Figure 3 shows the PS stack results before (A) and after (B) shear wave splitting correction, and also the fracture density and orientation (C) of the layer surrounding SH3. After shear wave splitting correction, the reflection events have been enhanced significantly by a more constructive stack for the radial component and minimized energy in the transverse component, while the fracture density and orientation can be used for azimuthal information in PP orthorhombic model building.

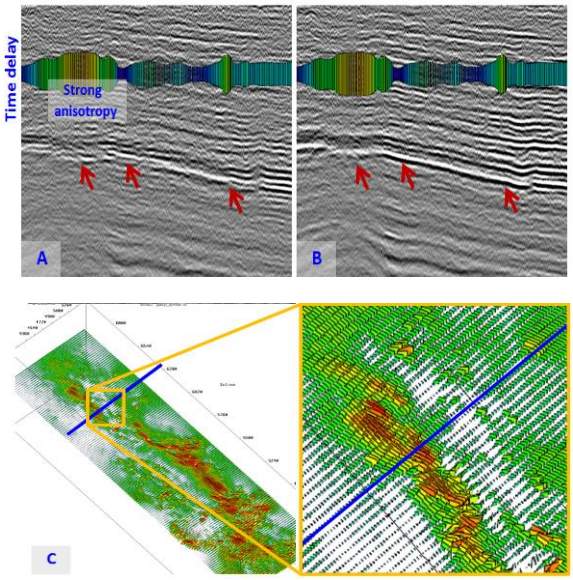

Figure 3: (A) PS stack without shear wave splitting correction; (B) PS stack after shear wave splitting correction; (C) Fracture density and orientation surrounding SH3.

PP-PS demultiple through MWD and SRME

For shallow-water data, it has become a common practice to first attack the short-period water layer-related multiples to reduce cross-talk among multiples and then followed by a conventional SRME to tackle the long-period surface-related multiples (Wang et al., 2014). In the PS data case, since shear waves do not pass through the water layer, multiples recorded in PS wave data mainly come from the source-side P wave while interbed multiples converted from P-S--P-S raypaths are relatively weak and typically negligible (Dragoset, et al., 2010). Also, P-wave velocity is typically twice as fast as S-wave velocity and therefore PS multiples contributed from the P-side will appear naturally closer to primaries in terms of moveout. This can make it difficult for algorithms that use residual moveout (ex., Radon de-multiple) to discriminate these multiples from the primaries. Conventional 3D tau-p deconvolution will also fail when the geology is complex and/or multiples cannot be differentiated from primaries by their periodicity. Therefore, we applied the model-based water-layer demultiple (MWD) approach proposed by Wang et al. (2014) to deal with the water layer-related multiples (Mw in Figure 4) in our PS data.

After removing most of the short-period water-layer-related multiples by MWD, we moved to SRME to handle the non-water-layer-related surface multiples (M1 and M2 in Figure 4). Compared to standard PP SRME for surface streamer data, there are two differences for SRME on OBC PS data: 1) the receivers are not on the surface as is required by

SRME; and 2) the multiple prediction needs to involve both PP and PS data. Therefore, we first used a double square root (DSR) normal moveout (NMO) equation combined with the water-layer Green's function to redatum the receivers from the water bottom to the surface for both PP and PS data. In the next step, the redatumed PP and PS data were convolved with each other to obtain the PS surface-related multiples with the timing for surface receivers, which were then redatumed back to the water-bottom receiver timing. Figure 5B shows the PS stack image after this two-step MWD and SRME flow. It is clear that multiples are effectively attenuated while primary events are well preserved.

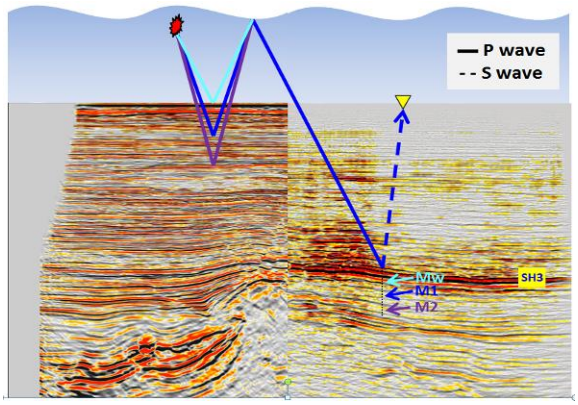

Figure 4: PP migration in PP time on the left and PS migration in PP time on the right.

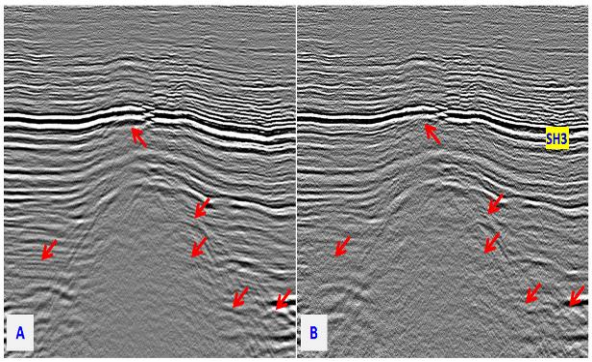

Figure 5: (A) PS stack before demultiple; (B) PS stack after demultiple.

Depth consistency between PP and PS images through PP/PS joint tomography

In PS depth migration, the mapping in depth to PP images is a well-known problem. Since PS reflections are non-reciprocal between source and receiver, it is typical that common reflectors of PP and PS do not match each other in depth. In addition, with an anisotropic medium, the errors in PS depth model building can be significant due to the higher sensitivity of PS waves to anisotropic parameters.

To tie PP and PS sections in depth, one conventional method is to pick major reflectors from the PP and PS images, and then use the mismatch between the horizons to invert for a new velocity model in a 1D approximation. We instead used the strategy proposed by Birkeland, et al. (2014) to update PS velocities through co-depthing of PP and PS horizons by S-ray tomography. We also incorporated dynamic warping to co-locate PP and PS images in a top-down fashion. As mentioned earlier, the reflectivity of PP and PS can be quite different in amplitudes. Instead of using the actual seismic data, instantaneous phase was chosen for dynamic warping due to its reduced sensitivity to amplitude variations. An example of the final PP and PS depth images is shown in Figure 6. The major horizons overall match well between PP and PS images even though many details still differ. For example, some strong impedance contrasts shown clearly in the PS image at the SH3 layer and the structures below SH5 are not evident in the PP image.

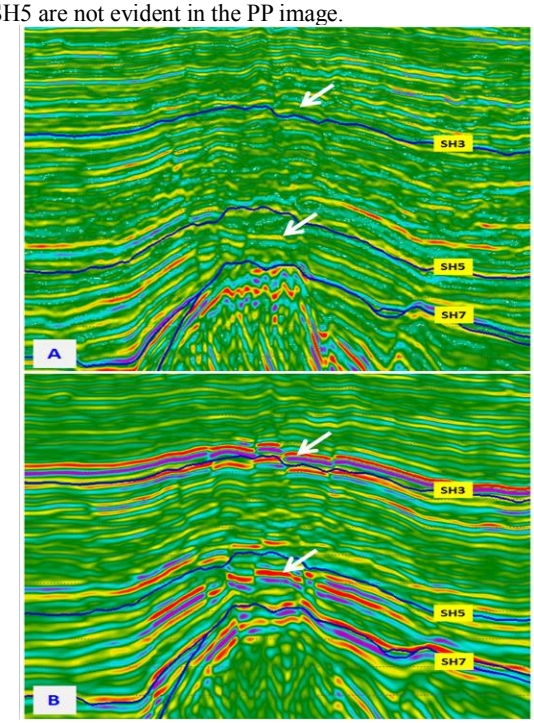

Figure 6: (A) PP final PSDM stack; (B) PS final PSDM stack.

Interpretation

Now that we have two consistent depth volumes, we can start to see the additional value from the PS image. As seen in Figure 6, the PS stack shows strong reflections below SH5 (Figure 6B) that is not in the PP stack (Figure 6A). An amplitude ratio map of PS/PP was computed between SH5 and SH7 (Figure 7A) and showed much higher values (yellow) in the prospective reservoir areas,

and note that they are coincident to the reservoir map (Figure 7B). These PS/PP amplitude ratio map values can acts as indicators of the lithology changes in the reservoir zone.

The Vp/Vs ratio can be used as a tool to help identify fluid types since seismic waves are sensitive to the saturating fluid type. For instance, with the increase of hydrocarbon saturation, the P wave velocity decreases while the S wave velocity remains relatively unchanged. The minimum Vp/Vs ratio was computed in the same layer from these data and showed a low Vp/Vs ratio in blue (Figure 7C). We excluded Vp/Vs ratios greater than 2 on the PS/PP amplitude ratio map (Figure 7D) to see if the strong amplitudes in the PS data are correlated to lower porosity. Furthermore, the contour of the amplitude map is similar to the reservoir map which might suggest some secondary Cuu Long oil fields.

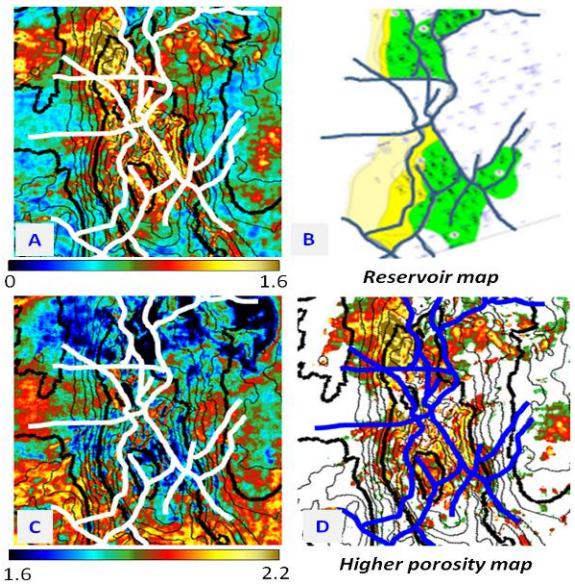

Figure 7: (A) PS/PP amplitude ratio map; (B) Reservoir map between the horizons of SH5 to SH7, green area represents the pay zones confirmed by wells; (C) Minimum Vp/Vs ratio map; (D) PS/PP amplitude ratio map of higher porosity rock.

Finally, in Figure 8 we demonstrate that with the addition of PS seismic data to PP seismic data, more reliable Vp/Vs ratios can be obtained through joint inversion of PP and PS rather than from conventional PP inversion alone. Figures 8A and 8B show an obvious mismatch between the inverted Vp/Vs ratios and well data when only PP seismic data is used for the inversion. Also Figures 8C and 8D display the Vp/Vs ratio values inverted from both methods versus Vp/Vs from well logs in a cross-plot. The PP+PS result has a 37.5% higher correlation to well data as compared to the PP inversion.

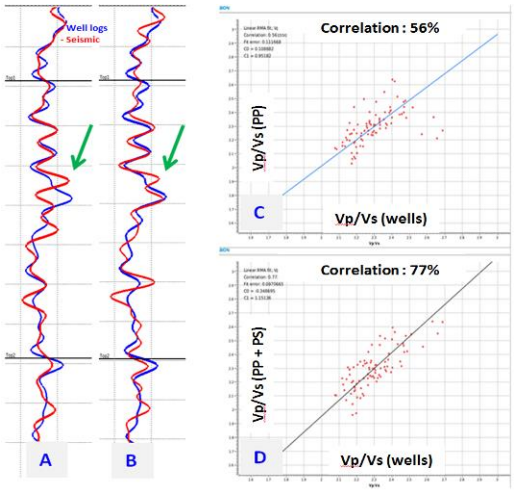

Figure 8: (A) PP only inverted Vp/Vs ratio; (B) PP + PS inverted Vp/Vs ratio; (C) Cross-plot and correlation coefficient between PP inverted Vp/Vs ratio and well data; (D) Cross-plot and correlation coefficient between PP+PS inverted Vp/Vs ratio and well data.

Conclusions

There are many areas like the Cuu Long Basin in Vietnam which still have lots of reserves left to be exploited. Detecting potential hydrocarbon reservoirs in clastic layers can be very challenging using PP wave seismic data alone. (Converted) PS wave data provides needed complementary information. However, there are many processing issues to be addressed to get high quality reliable PS images. In this paper we showed new processing workflows and technologies to improve PS seismic quality, resolution, and depth consistency, so that it can be used directly together with PP seismic data for interpretation studies.

In addition, PS wave seismic data can provide extra information and help to reduce risk or uncertainty. Shear wave splitting analysis can help determine fracture density and orientation, whereas joint PP-PS inversion can provide better and more reliable attributes such as Vp/Vs ratio to delineate high-grade prospective hydrocarbon plays. With the new flow providing good quality and consistent depth volumes, the PS/PP amplitude ratio and the Vp/Vs ratio maps from this Cuu Long Basin survey conform to the interpretations of the existing pay zones with some indications of potential alternative target zones.

Acknowledgments

We would like to thank Vietsovpetro and CGG for permission to show this work. We are also grateful to Jim Keggin from SBGS and Stephane Fintz from CGG programming department whose shared wisdom and knowledge are aggregated in this paper.